Chapter 8
Hydrodynamic Optimisation of a Containership and a Bulkcarrier for Life-Cycle Operation

George Zaraphonitis, Aggeliki Kytariolou, George Dafermos, Scott Gatchell, and Anders Östman

Abstract Efficient ship operation has always been a challenge of paramount importance to the ship owner, aiming to minimize operational expenditures and to maximize annual revenues. Nowadays, efficient ship operation is even more important due to the global warming phenomenon and the urgent need to reduce greenhouse gas emissions, next to the fuel cost. In the present chapter, we consider the possible retrofitting of two existing vessels, namely a bulk carrier and a container ship, on the basis of results of conducted hydrodynamic optimizations. For both vessels, bulbous bow and operational trim optimizations were carried out using advanced CFD tools. In addition, a weather routeing tool was developed and applied to the operation of both vessels, assuming realistic operational conditions and online weather data, while aiming at the reduction of fuel oil consumption.

Keywords Life-cycle cost · Optimization of operation · Trim optimization · Hullform optimization · Weather routeing · Ship routeing

G. Zaraphonitis (✉) · A. Kytariolou · G. Dafermos
Ship Design Laboratory, National Technical University of Athens, Athens, Greece
e-mail: zar@deslab.ntua.gr

A. Kytariolou
e-mail: akytariolou@deslab.ntua.gr

G. Dafermos
e-mail: dafermos@deslab.ntua.gr

S. Gatchell
Hamburger Ship Model Basin, Hamburg, Germany
e-mail: Gatchell@hsva.de

A. Östman
Ship and Ocean's Structures, SINTEF Ocean, Trondheim, Norway
e-mail: Anders.Ostman@sintef.no

A. Papanikolaou (ed.), *A Holistic Approach to Ship Design*,
https://doi.org/10.1007/978-3-030-71091-0_8

Abbreviations

CAESES®	Computer Aided Engineering System Empowering Simulation by FRIENDSHIP SYSTEMS AG, Germany
CFD	Computational Fluid Dynamics
ECAs	Emission Control Areas
EEDI	Energy Efficiency Design Index
EEOI	Energy Efficiency Operational Indicator
FreSCo$^+$	RANSE solver by HSVA and Technical University Hamburg
HSVA	Hamburg Ship Model Basin
IMO	International Maritime Organization
LOA	Length over all
LBP	Length between perpendiculars
MARPOL	International Convention for the Prevention of Pollution from Ships
MEPC	IMO's Marine Environment Protection Committee
NAPA	Naval Architecture Package for ship design by NAPA Oy, Finland
NEWDRIFT	3d potential flow, panel code for seakeeping analysis of ships and floating structures by NTUA
NTUA	National Technical University of Athens
RANSE	Reynolds-averaged Navier-Stokes equations
SEEMP	Ship Energy Efficiency Management Plan
SFOC	Specific Fuel Oil Consumption
ShipX	A comprehensive workbench by SINTEF Ocean, containing a variety of marine hydrodynamic analysis tools
SINTEF	SINTEF Ocean
TEU	Twenty Feet Equivalent Unit (container)

8.1 Introduction

Efficiency of ship operation is a challenge of comparable importance to ship design optimization, aiming to improve ship's performance, to reduce fuel cost and to ensure ship's safety and environmental protection, with the ship operating in a highly competitive market such as international shipping. While the latter was always a key priority for the ship operators, it can be argued that the importance of environmental protection was not realized for many years. A major step towards the protection against environmental pollution from shipping operation was the introduction of MARPOL (International Convention for the Prevention of Pollution from Ships) by IMO in 1973. Since then, many things have changed in maritime operations as the impact of climate change has been gradually recognized and is nowadays and universally acknowledged. Trying to respond to the increased societal concern, international or intergovernmental organizations, such as IMO or the European Union,

national governments and regulators are setting into force specific regulations against pollution, setting hard constraints on polluting activities, or introducing incentives for greener operation and penalties to those not able or not interested to comply.

With global warming being the most important environmental concern, IMO issued a series of important regulations, aiming to reduce greenhouse gas emissions from ships. The introduced Energy Efficiency Design Index (EEDI) is applicable to all new ships and aims to reduce GHG emissions from shipping by design measures, i.e. by promoting the design and construction of more energy efficient ships. Ship Energy Efficiency Management Plan (SEEMP) on the other hand, which is mandatory both for new and existing ships "is an operational measure that establishes a mechanism to improve the energy efficiency of a ship in a cost-effective manner. The SEEMP also provides an approach for shipping companies to manage ship and fleet efficiency performance over time using, for example, the Energy Efficiency Operational Indicator (EEOI) as a monitoring tool". Both EEDI and SEEMP have been introduced by IMO resolution MEPC0.203(62), adopted in July 2011.[1]

With the freight rates persistently oscillating during the last 12 years around a small fraction of their 2007 and 2008 peak values[2] and with the fuel cost being the most important annual expenditure, reduction of fuel consumption would be of vital importance for ship operators, even without its paramount environmental impact and the need to comply with regulatory requirements. Considering the above, a study dealing with the operational optimisation of two widely used vessel types, namely a bulk carrier and a container ship was considered an essential Application Case of the HOLISHIP project. More specifically, the objectives of this Application Case and of the present book chapter were to investigate for two sample ships possible retrofitting solutions, including hullform modifications and/or the installation of energy saving systems and equipment, along with operational measures, such as trim optimization and route optimization, all aiming to reduce fuel oil consumption.

The sample ship characteristics, the optimization of ships' hull form and of their operation in calm water and under realistic environmental conditions, the tools that were developed or adjusted and the obtained results will be presented in the following sections.

8.2 The Sample Vessels

Two representative vessels, a 4235 TEU Cellular Container Ship operated by DANAOS and a Newcastlemax Bulk Carrier, operated by Star Bulk have been selected as the testbeds for the development and testing of the procedures and tools used in the HOLISHIP project for the optimisation of the operational performance of

[1] International Maritime Organisation (IMO), Energy Efficiency Measures, https://www.imo.org/en/OurWork/Environment/PollutionPrevention/AirPollution/Pages/Technical-and-Operational-Measures.aspx.

[2] See for example Baltic Exchange Dry Index, https://www.balticexchange.com.

typical merchant vessels. The main characteristics of the sample container ship are presented in Table 8.1. The ship is operating between East Mediterranean and USA via the Gibraltar straights, calling at the following ports: Ashdod, Haifa, Piraeus, Livorno, Genoa, Valencia, Halifax Nova Scotia, New York, Norfolk, Savannah, Valencia, Tarragona, Livorno and Ashdod.

The main characteristics of the sample Bulk Carrier are presented in Table 8.2. This ship is usually operating between South America and China: transit of Atlantic to Cape Town, transit of Indian Ocean, bunkering stop in Singapore (18 h) and transit through the Taiwan Strait to the gulf of Beihai in China. Alternative areas of operation of this ship are: North Australia to China and South America to Rotterdam.

Based on the 2d lines plan provided by the collaborating ship operators, 3d models of the hullform of each vessel were developed first in NAPA® and subsequently transferred to CAESES® (Figs. 8.1 and 8.2). In the case of the bulk carrier, a variant of its hullform has been created by adding a bulbous bow. Subsequently, the 'Free Form Deformation' tool provided by CAESES® to facilitate the variation of the bulbous bow form of the container ship and of the modified bulk carrier. To this end, a series of control points is added, located within a cube enclosing the area of the hull (here: bulbous bow), which is to be varied (Fig. 8.4). The control points located at the two aft layers and the two upper layers are kept at their original position, in order to ensure continuity of the surface, while some of the remaining control points are translated in space at selected directions resulting in a deformation of the

Table 8.1 Main characteristics of the container ship *ZIM LUANDA*

DWT (summer)	50,829
GT/NT	40,030/24450
L_{OA}	260.049 m
L_{BP}	244.80 m
Beam	32.25 m
Depth moulded	19.30 m
Draft (summer)	12.60 m
No. of holds/hatches	Seven (7)/Sixteen (16)
Nominal container capacity	4253 TEU
Reefer containers	400 UNITS
Homogeneous 14MT/TEU	2900 TEU
Main engine	HSD MAN B&W 8K90MC-C
MCR	49,680 BHP
Generators	4 X 1700 kW
Bow thruster	1 × 1600 kW
Speed	Abt 24.5 kn
Class	DNV GL

Table 8.2 Main characteristics of the bulk carrier *Star Marisa*

DWT (scantling)	208,000
GT/NT	106,900/66145
L_{OA}	299.88 m
L_{BP}	294.00 m
Beam	50.00 m
Depth moulded	25.00 m
Draft (D.L.W.L.)	16.10 m
Draft (Scantling)	18.50 m
No. of Holds	Nine (9)
Main Engine	MAN 6G70ME-C (Mark9.2) Tier II
SMCR	17,494 KW @ 78.7 RPM
Service Speed	Abt. 14.5 kn (CSR with 15% sea margin in design draft)
CLASS	BV

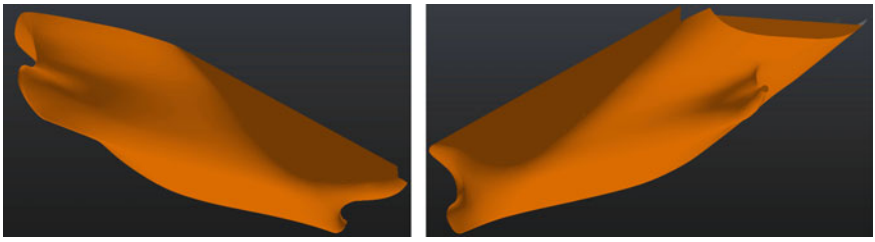

Fig. 8.1 3d model of the hullform of the container ship in NAPA®

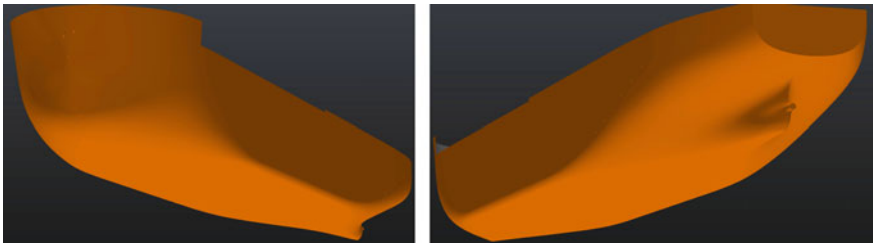

Fig. 8.2 3d model of the hullform of the bulk carrier in NAPA®

selected part of the hull. The translation of the control points is controlled by a set of variables. By assigning suitable values to these variables, the user can achieve the desired hullform deformation (Fig. 8.3).

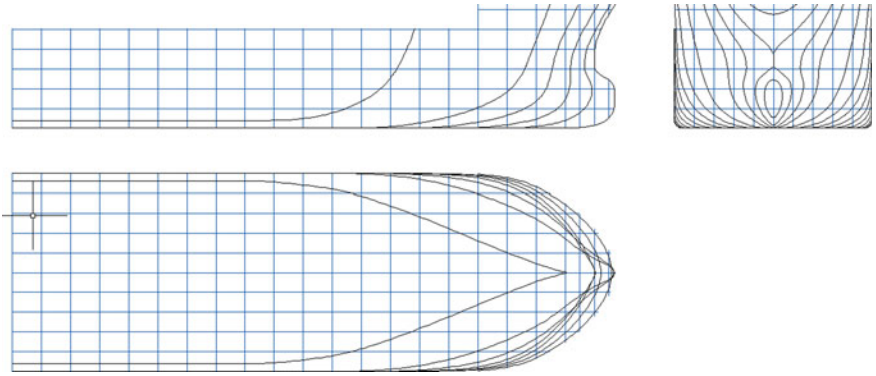

Fig. 8.3 Lines plan of modified bulk carrier bow

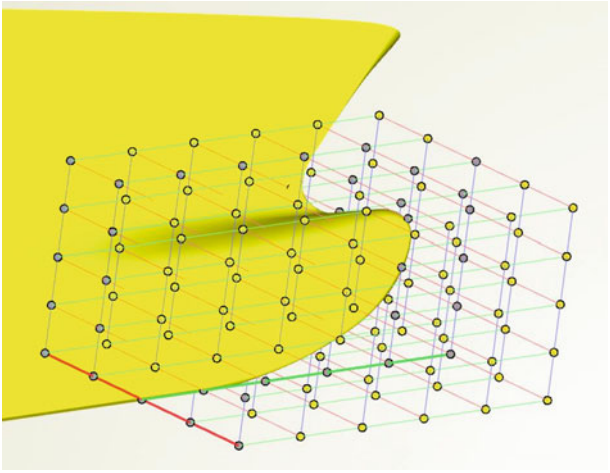

Fig. 8.4 Bow area of the container ship with the control points used for the bulb transformation

8.3 Hullform and Operational Optimization of a Container Ship

To support operational optimization and the possible retrofit process, HSVA performed a series of computations regarding the resistance and propulsion performance on a selection of hull form variations. These computations rely on the appropriate tool for the level of detail needed for the corresponding stage of development. At the initial stage, potential-based, panel code analysis tools were used. Such tools provide a fast, but moderately accurate overview of ship's performance. The information gained through these simple tools facilitates a narrowed selection of design characteristics for further optimization. At the later stages, more sophisticated and more

time-consuming tools provide greater detail, and thereby distinguishing between subtle hull form changes, in order to reach the final design.

The ship under investigation is the container ship presented in Table 8.1.For this vessel, HSVA investigated the trim optimization, the bow shape optimization, and a combination thereof. The results were also used by other HOLISHIP partners for further investigation with regards to machinery retrofitting for reducing fuel oil consumption, and for the development and application of a weather routeing tool.

The first stage of the conducted investigation examined the (hydrodynamic) operational optimization of the container ship. No geometry changes were considered in this first stage and the original ship hull form was used. Instead, the investigation considered the simple change in loading, to produce a static trim, and the subsequent effect on the ship resistance and propulsion at a range of sailing speeds. In the second stage of the investigation, hull form variations were introduced. Initially, a search space consisting of 3 design parameters was applied. These design parameters correspond to the length of the bulbous bow, its width at the forward perpendicular and the height from baseline of its foremost point. Later, the search space was expanded to 5 design parameters adding the so-called upturn and fullness parameters. The upturn parameter can be used to modify the inclination of the upper part of the bulb's profile while with the fullness parameter the vertical centre of area of the bulb's transverse section can be shifted upwards or downwards. The hull form variations were limited to the bulbous bow. The operational conditions reflected the even keel loading condition at the design draft and the new (reduced) design speed of 18 knots. In the third stage, the combined effects of the first two stages were considered. The goal of each of the investigations was to determine the hull form and operating point for the lowest propulsion power requirement.

Before any computations could commence, the issue of some missing pieces needed to be resolved. The description of the hull form did not include a geometric description of the rudder, nor of the propeller. For the rudder, an approximation was created in CAESES®, based on 2-dimensional diagrams provided by the ship owner. A simple NACA profile was used in lieu of the actual rudder geometry. While this may have some effect on the absolute resistance and propulsion performance of the ship, the relative comparison between hull form variations was deemed adequate for the purpose of this investigation. A surrogate propeller was selected from the database of stock propellers available at HSVA for use in the investigation. As with the rudder, although an absolute powering performance is not reachable, the relative improvement between designs was also deemed adequate. At this point, a sufficient geometry description was reached, allowing the numerical analysis to begin in earnest.

The first step was to establish the computational domain. The free surface and the propeller region were of particular interest for the computations. The best practice guidelines at HSVA prescribed a finer mesh resolution in these regions to better capture flow details. The resulting meshes contained approximately 11.3 million hexahedral cells. The extent of the computational domain is presented in Fig. 8.5. As a basis for the subsequent optimization exercises, HSVA performed a series of calm water resistance and propulsion computations for the ZIM LUANDA container

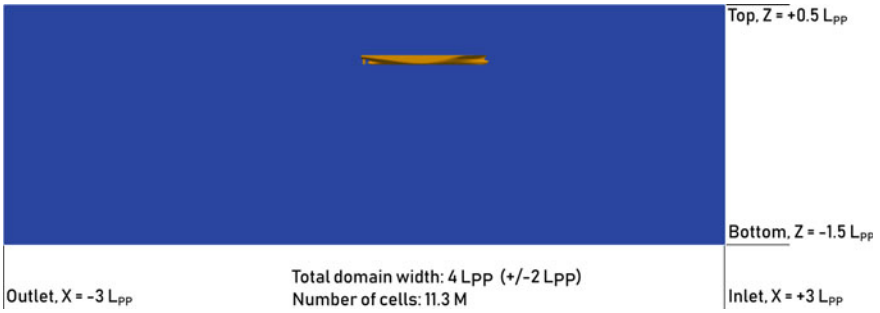

Fig. 8.5 Computational mesh for the case of the container ship

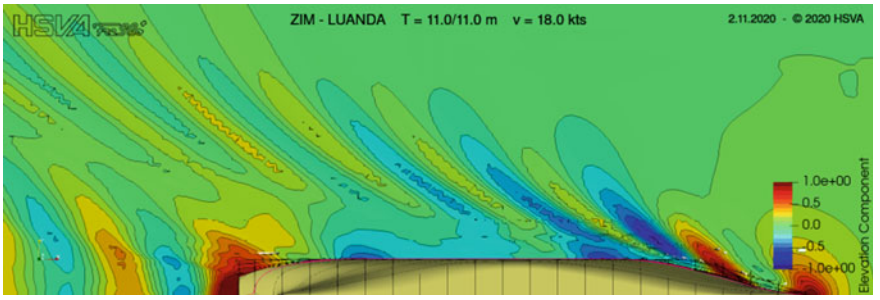

Fig. 8.6 Wave field, viewed from above for the original hullform at zero trim at 18 kn

ship. These computations cover a speed range from 12 to 24.5 knots for the ship at the even keel, designed loading condition of 11.0 m draft. Typical visualizations of the obtained results are shown in Figs. 8.6 and 8.7.

In an initial round of computations, the ship was computed over varying speeds: 18, 20, 22, 24 knots and varying hydrostatic trim conditions: 1 m by Stern, Even Keel, and 1 m by Bow. The results verified that the hydrostatic trim condition of 1 m by the bow is the best of the three conditions over all speeds computed. However, the optimal condition for each speed had not yet been determined. This merely indicated which side to explore in finer resolution. The second round of computations extended the trim to 2 m by the bow, as well as some intermediate steps. In general, a static trim of 1.5 m bow down gives the optimal power performance improvement between 2 and 3% over the speed range and draft, as shown in Fig. 8.8.

The next stage of the study was the bulbous bow optimization. The software platform CAESES® provided the means to modify the bulb geometry by way of the Free Form Deformation Tool. For this study, a series of calculations with ν-Shallo, the HSVA's in-house panel code for wave resistance was carried out, using equidistant spacing of the five design parameters (namely the bulbous length, width, height, upturn and fullness). The obtained results were used as the basis for the creation of a Response Surface Model (see Marzi et al. 2018), enabling the fast evaluation of

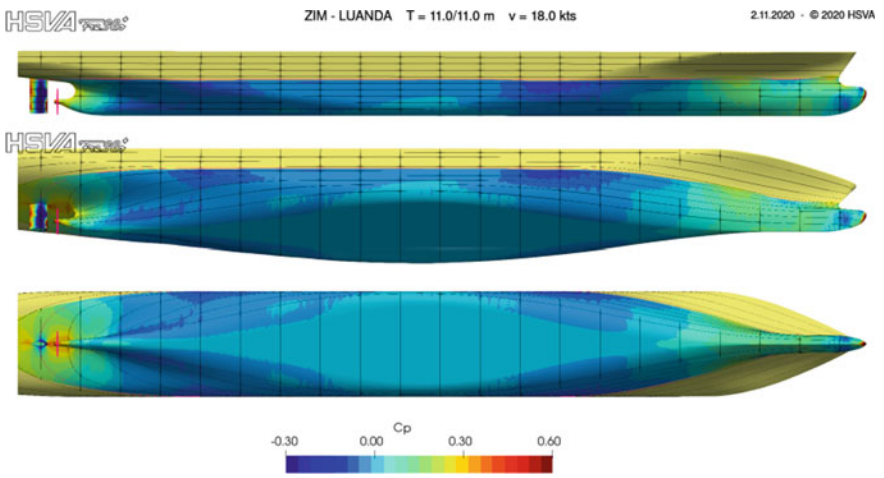

Fig. 8.7 Pressure distribution (Cp) on hull for different view angles, original hullform at zero trim at 18 kn

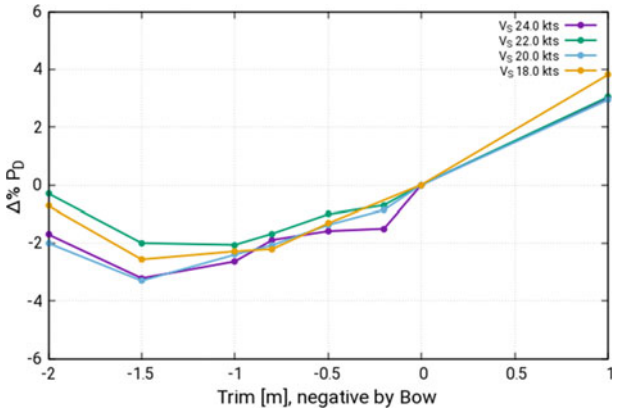

Fig. 8.8 Trim optimisation results for the original hull form of the container ship at 11.0 m draught and a speed range from 18 to 24 kn (negative trim corresponds to bow down)

alternative hullforms replacing computationally demanding CFD calculations. Then, a formal optimization of the bulbous bow was carried out using a Tangent Search optimization algorithm along with the Response Surface Model instead of CFD calculations. The verification of the performance of the optimum hull was carried out using HSVA's in-house tools, i.e. the panel code ν-Shallo and the RANSE code FreSCo$^+$ (Gatchell et al. 2000; Hafermann 2007). A comparison of the performance of the original (baseline) hullform and the optimized one is presented in Fig. 8.9 and Table 8.3. As can be observed from Table 8.3, in comparison with the baseline the total resistance of the optimized design is reduced by 4.8% according to the ν-Shallo

Fig. 8.9 Comparison of wave profile around the baseline and the optimized bulbous bow

Table 8.3 Comparison of resistance and propulsion power for the baseline and the optimized bulbous bow at zero trim

	R_t (potential flow code) [kN]	R_t (viscous flow code) [kN]	P_D [kW]
Baseline	742.59	804.1	10294
'Best'	706.7 (−4.8%)	780.6 (−2.9%)	9982 (−3.0%)

Table 8.4 Comparison of propulsion power for the baseline and the optimized bulbous bow at zero and optimum trim

	P_D at Even Keel [kW]	Optimum Trim (negative bow down)	P_D at Optimum Trim [kW]
Baseline	10294	−1.5 m	10002 (−2.8%)
'Best'	9982 (-3.0%)	−1.0 m	9867 (−4.1%)

results and by 2.9% according to the results of the RANSE viscous calculations with FreSCo+. The propulsion power, calculated with FreSCo$^+$ and QCM (the propeller Vortex Lattice Method QCM developed at HSVA) is reduced by 3% in comparison with the baseline. Calculations with the optimized design at the optimum trim (1.0 m bow down) resulted in a propulsion power of 9867 kW, i.e. a total reduction of 4.1% in comparison with the baseline (Table 8.4).

8.4 Hullform and Operational Optimization of a Bulk Carrier

The optimisations studies on the Newcastlemax Bulk Carrier consisted of the optimisation of the bulbous bow fitted to the modified bulk carrier's foreship, along with a trim optimisation of the original vessel without bulbous bow. Both studies were performed at the design speed of 14.5 kn. The vessel resistance was computed using the FINE^{TM}/Marine CFD solver (Deng et al. 2005, 2015). The CFD simulation was set up to account for the effect of the propulsion force on the dynamic trim of the vessel. This was done by applying a body force model, setting thrust force equal

to the computed resistance at the position of the propeller, acting in the direction of the propeller axis. The propeller force was therefore accounted in the computation of the hydrodynamic force balance of the vessel. The vessel resistance was computed assuming a smooth hull surface, while the additional resistance component due to hull roughness was added in a subsequent post processing step, in a similar procedure as applied to model test data obtained from physical experimental towing tests. The resistance from the CFD simulation is used as input to the ShipX Speed and Power module. ShipX, developed by SINTEF Ocean, is a comprehensive workbench containing a variety of marine hydrodynamic analysis tools, such as speed prognosis, stations keeping, sea keeping analysis, etc. The ShipX Speed and Power module computes the required shaft power necessary to maintain a given speed. In addition to the computed resistance from the CFD simulations, the module also takes the propulsion efficiency into account. The computed nominal wake at the location of the propeller plane is extracted from the CFD simulations and used as input to the ShipX module when the propulsion efficiency is evaluated.

The size of the computational domain is based on the length overall of the ship (L_{OA}). The upstream inlet boundary is located $1.5L_{OA}$ in front of the vessel, the downstream outlet boundary is located $3L_{OA}$ behind it, while the far field side is located $2L_{OA}$ from the centreline. The bottom boundary is located $1.5L_{OA}$ below the undisturbed water surface and the top boundary is located $0.6L_{OA}$ above the water surface. By applying a symmetry boundary condition at the centreline, the computational domain is reduced to only include the port side of the vessel. The computational mesh was generated using the HEXPRESS mesh generator, which is part of the FINE^{TM}/Marine CFD package. The total number of grid cells was about 4.5 M. The computational domain and mesh at outer boundaries are visualised in Fig. 8.10. The turbulence model used in the RANS simulations was the k-ω SST model. The free surface interface was captured using the VOF technique.

The Sobol sensitivity analysis method, as implemented in the CAESES® optimisation software, was used to sweep the parameter space to identify combinations of design parameters that result in a low value of required shaft power. To find the local minimums, refined optimisation must be conducted in the vicinity of the location of the local minimums. The global minimum can thereafter be found as the minimum of the local minimums.

A set of simulations was conducted for the original vessel without bulbous bow, with variation of trim angle while keeping the displacement constant. The trim angle ranges from -2 to $+2°$ where a positive angle means a bow down trim. The required power as a function of trim angle is presented in Fig. 8.11. The lowest required power was equal to 12390 kW, corresponding to a trim angle of 0.25°. The even keel trim angle resulted in a required power of 12523 kW. Thus, by trimming the vessel 0.25° bow down, the required power is reduced by 1%.

A modified version of the bulk carrier was designed by adding a bulbous bow. The shape of the bulb was parametrized in CAESES®, using the Free Form Deformation tool. Shape parameters describing the length (L_{bulb}), thickness (T_{bulb}), vertical extent

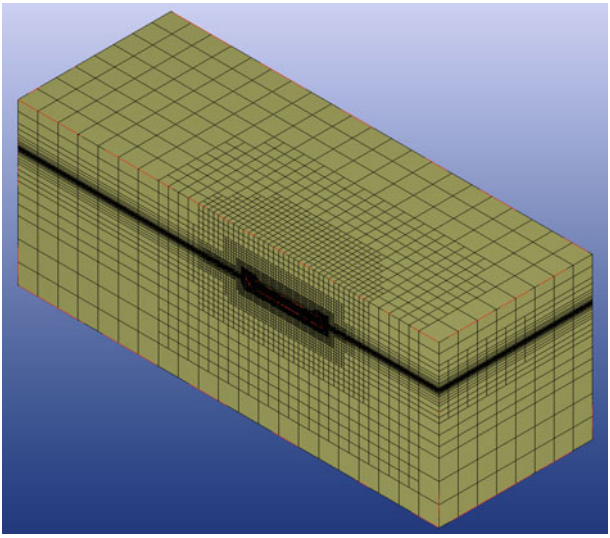

Fig. 8.10 Computational mesh for the case of the bulk carrier (4.5 Mio cells)

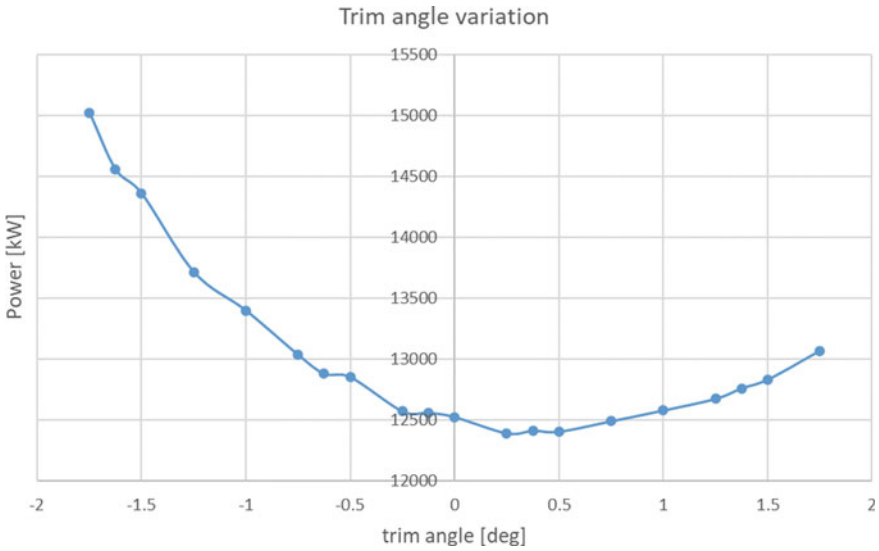

Fig. 8.11 Required shaft power as a function of trim angle for the original bulk carrier (positive trim: bow down)

Table 8.5 Lowest computed required power and bulb shape parameters for each tested trim angle

Trim angle	L_{bulb}	T_{bulb}	VE_{bulb}	VP_{bulb}	P [kW]
0° (even keel)	−0.125	0.44375	0.9875	0.328125	12412
0.125°	−0.75	0.5375	1.175	−0.21875	12414
0.25°	2.5	0.475	0.95	0.5625	12427

(VE_{bulb}) and vertical position (VP_{bulb}) of the bulb were defined and used to create bulb shape variations. A set of 35 bulb variations were defined using the Sobol sampling method.

The displacement at even keel loading condition was set to be the same as for the original vessel design without bulbous bow. The computed power varies from 12412 kW to 12574 kW. The vessel with the bulb that requires the lowest power is about 1% better in terms of power consumption than the original vessel without bulb at even keel loading condition (computed to 12523 kW). However, the best bulb found does still require marginally more power than the vessel without bulb at optimum trim loading condition (computed to 12390 kW at 0.25° trim angle). The reason for the reduced propulsion power of the trimmed vessel could be the reduced submergence at the aft, and therefore reduced wetted transom area, which results in a reduction of pressure/wave resistance contribution from the aft ship.

To further investigate this, a set of simulations with forward still water trim angle was conducted. Simulations were performed for 0.125 and 0.25° forward trim. For each of the forward trim angles, a Sobol sequence was defined with 20 variations of the bulb design variables. The result for the best bulb in each set of simulations is presented in Table 8.5. The minimum required power is still found for the even keel condition, although the simulations at 0.125° forward trim resulted in practically the same required power, with only 2 kW difference. It is possible that, although the resistance component from the aft ship is reduced by trimming forward, the increased submergence of the bulb makes the bulb less effective and the total resistance is increased. It is also possible that by expanding the set of simulations with forward trim angle, an improved bulbous bow design, with further reduced shaft power can be found.

The wave pattern of the original vessel without a bulbous bow is compared at 0.25° forward trim against the even keel (0°) loading condition (Fig. 8.12). As may be observed in this figure, the elevation of the transom stern wave crest height is reduced in the simulation with the forward trim. Also, the wave trough at the aft shoulder is reduced. At the same time, due to the increased submergence of the bow, an increased wave trough is observed at the forward shoulder. But, overall, the resistance computations show that the benefit from the improved aft ship wave pattern outweighs the worsening of the wave pattern at the forward shoulder of the ship. In Fig. 8.13, the wave pattern generated around the ship equipped with the best bulbous bow found at even keel loading condition is compared against the wave pattern generated by the original vessel without bulb. The bulb generates a more

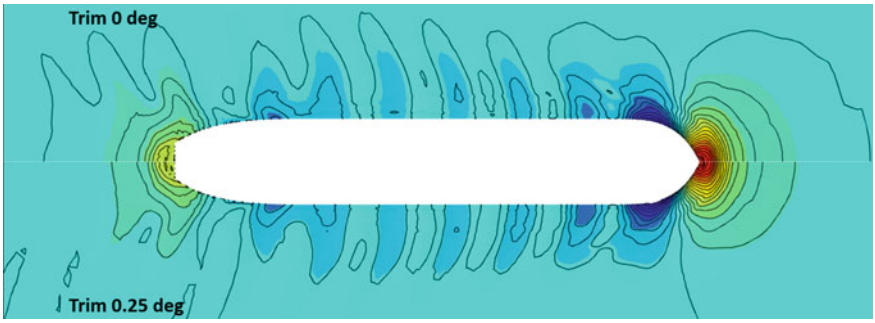

Fig. 8.12 Free surface wave pattern. Comparison of even keel loading condition (above) against 0.25° forward trim loading condition (below)

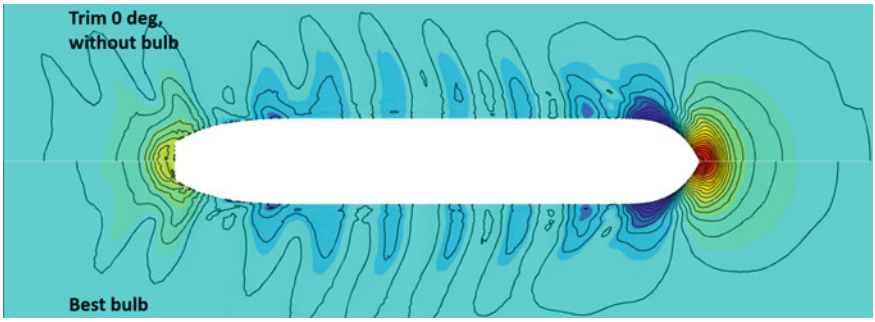

Fig. 8.13 Free surface wave pattern. Comparison of base case without bulb (above) against best bulb found for even keel loading condition (below)

favourable forward shoulder wave with reduced wave trough. Also, as expected since both simulations are performed at even keel loading condition, the aft ship wave pattern is very similar.

8.5 Weather Routeing

8.5.1 Development of a Ship Routeing Tool

In the framework of the HOLISHIP project a new ship weather routeing tool was developed and used for the operational optimization of the sample vessels, the container ship and the bulk carrier. The ship-routeing tool was developed in Matlab®, making use of the numerous functions and toolboxes available.

Matlab® combines a desktop environment tuned for iterative analysis and design processes with a powerful programming language. Users are provided with a variety

of toolboxes, which are professionally developed and rigorously tested. The mapping toolbox in particular, that is widely used for the development of the ship-routeing tool, provides algorithms and functions for analysing geographic data and creating map displays in Matlab®. Users can import vector and raster data from a wide range of file formats and web map servers. Vector and raster data can even be displayed together as needed.

The geographic data is in vector format and is referred to as a vector map. This format consists of specific points, along with some indication as to how they should or should not be connected to each other. In the mapping toolbox, vector data consists of sequentially ordered pairs of latitude and longitude coordinates. A map projection displays the surface of a sphere (or spheroid) in a two-dimensional plane. There are many different ways to project a map, but in all cases, various types of distortions are introduced. Maps oriented for sea navigation commonly use Mercator projection which is adequately efficient as long as the route of interest is located at a safe distance from poles, where distortion is high. For regions near poles, it is more suitable to revert to conic or azimuthal projection. The ship-routeing map can be enriched by adding relevant raster data and 3d displays can be created. Such kind of data may correspond to surface (land) elevation and bathymetry layers. The simplest way to display raster data is to assign colours to matrix elements according to their data values and plot them in two dimensions.

After setting up the map environment, the next step was to develop an algorithm in Matlab®, which would be used to plan alternative ship routes and display them on the map. A route is defined by its starting and end points along with a number of n intermediate waypoints. These points can be given directly by the user either by clicking on the map or by typing their exact coordinates. Moreover, these points can also be read from an external file. This group of points create $n + 1$ legs, each one of which can be handled and analysed separately. For instance, for each point along the route it is possible to calculate water depth, or its distance from the nearest coast, or to check whether it lies within specific areas (for example within an Emission Control Area (ECA), or a possibly dangerous or non-permitted area). Apart from being defined by the user, the coordinates of n intermediate waypoints can be also selected randomly, or by an optimization algorithm so that it is possible to generate and analyse automatically a large number of routes, connecting the same starting and end points at almost zero computing time. The user can specify a series of constrains, such as minimum distance from coast, minimum depth along the route, time spent or distance travelled within Emission Control Areas, avoidance of non-permitted areas etc. Any route that doesn't comply with the given constrains is considered unfeasible and is neglected from the process, whereas feasible routes are stored for further analysis.

Weather forecast data along any route can be readily imported by a variety of sources, enabling the user to perform seakeeping analysis along the suggested routes. To this end, detailed seakeeping calculations for the vessel in question at various loading conditions, speeds of advance and for a range of incident waves are carried out beforehand and the results are stored in a database to be used during the ship route optimization. By doing so, the evaluation of the performance of a ship along

a route can be considerably faster, while at the same time the ship routeing tool is completely de-coupled from the software tools that maybe used for the seakeeping calculations and it is therefore possible to use seakeeping results from any available source.

Reliable weather predictions, as possible for the whole duration of the crossing, are essential in order to be able to evaluate and compare the performance of a ship along alternative routes. The routeing tool can access such data from various weather prediction providers, including Copernicus Marine Environment Monitoring Service (https://marine.copernicus.eu), providing a 7-days forecast, or the weather forecast platform SKIRON, developed and maintained by the University of Athens, School of Physics (https://forecast.uoa.gr/) providing a 7-days forecast horizon. Forecast data from Copernicus are available at a spatial resolution of $0.083° \times 0.083°$ and temporal resolution of 3 h for waves, spatial resolution of $0.025° \times 0.025°$ and temporal resolution of 24 h for currents and spatial resolution of $0.025° \times 0.025°$ and temporal resolution of 6 h for wind predictions. Forecast data from SKIRON are available only for waves, at a spatial resolution of $0.5° \times 0.5°$ world-wide, while a much finer resolution of $0.05° \times 0.05°$ is used within the Mediterranean. All data are in GRIB[3] format and a suitable code in Matlab® has been prepared to read all the components that are needed for the analysis. From the various types of data included in the weather predictions, the most important ones for the routeing tool are the wave height, mean period and direction. Relevant data regarding sea currents predictions are obtained from Copernicus Marine Environment Monitoring Service.

Integration of the ship-routeing tool with optimization algorithms available in Matlab® enables the user to optimize the ship route according to appropriate optimization criteria, each time selected by the user. In addition, relevant constraints on the ship motions and accelerations along the route can be introduced, aiming to ensure safety of operation and acceptable comfort standards for the crew.

8.5.2 Container Ship Weather Routing Optimization

The 4235 TEU container ship operated by DANAOS has been extensively used as a testbed for the development of the routeing tool, namely to test its potential for the operational optimization of the ship and the minimization of the annual fuel consumption. The ship is serving a route starting from the Ashdod and Haifa ports in Israel, then sailing via Piraeus, Livorno, Genoa and Valencia in the Mediterranean and through the Strait of Gibraltar, it crosses the Atlantic heading Halifax in Nova Scotia, Canada and from there proceeding to New York, Norfolk and Savannah. From there it returns to Valencia, Tarragona, Livorno and finally to Ashdod. Apart from its typical route, the ship has been tested in many other areas of operation, using available weather predictions, as well as recorded weather data in order to

[3]GRIB files are a special binary format, commonly used in meteorology to store historical and forecast weather data.

test and validate the potential of the routeing tool. The objective function used in most of these studies was the minimization of the fuel consumption, while a set of constraints on the ship motions and accelerations along the route have been applied. For the evaluation of the fuel consumption a series of software tools have been used for the calculation of calm water resistance, the added resistance in waves, the wind resistance and the modelling of the propeller and main engine.

For the calm water resistance, calculations were carried out by HSVA, using the CFD code FreSCo+ (Hafermann 2007). FreSCo^{+} is a RANSE (Reynolds-Averaged Navier-Stokes Equations) solver jointly developed by HSVA and Technical University Hamburg since 2005, based on a finite volume method and is capable of handling fully unstructured polyhedral meshes. For the added resistance in waves as well as for the evaluation of the ship motions in waves, the NEWDRIFT+ code is used. NEWDRIFT + is a 3d panel code based on Green Function's method, developed by NTUA, which can be employed for the evaluation of motions, wave loads and mean second-order forces on ships and floating structures subject to incident waves in the frequency domain (Papanikolaou, 1985, Papanikolaou and Zaraphonitis, 1987, Papanikolaou and Schellin, 1992). The original version of NEWDRIFT calculates the second-order drift forces of a ship or a floating object at zero forward speed based on direct integration over the wetted surface (near field method). However, for ships with forward speed a variation of the far field method is developed and used in NEWDRIFT+ for the calculation of added resistance (Liu et al. 2011). In addition, a simplified formula proposed by Liu and Papanikolaou (2015) for the calculation of added resistance of ships in waves can also be used. A comparison of numerical predictions with experimental measurements for two well-known and extensively studied vessels, i.e. the KVLCC2 ship and the S175 container ship is illustrated in Figs. 8.14 and 8.15 extracted from Liu and Papanikolaou (2015).

Using NEWDRIFT+, extensive calculations have been carried out for a series of loading conditions, ship speeds, headings and wave lengths assuming regular

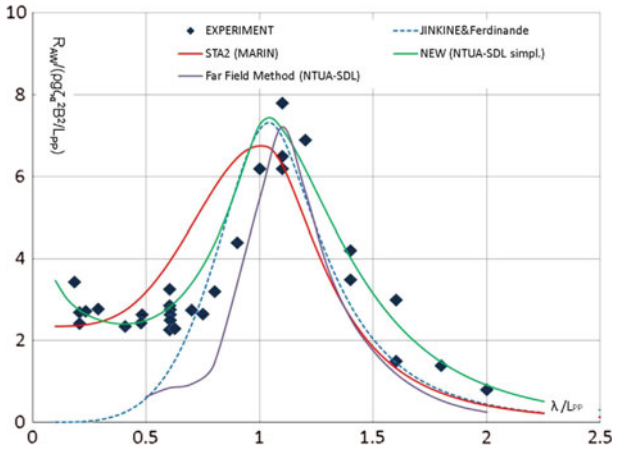

Fig. 8.14 Added resistance of KVLCC2 ship in head waves at Fn = 0.142

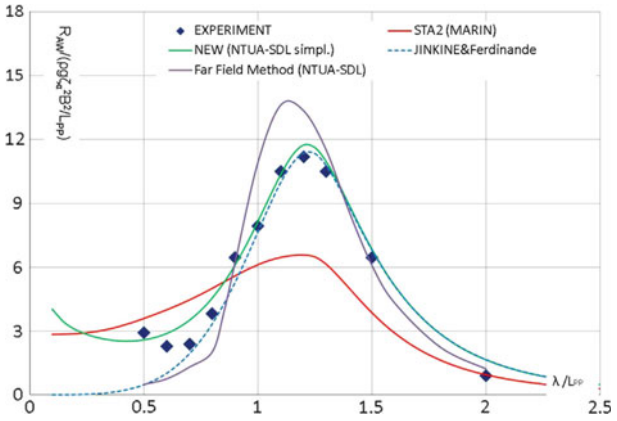

Fig. 8.15 Added resistance of S175 container ship in head waves at Fn = 0.275

waves. Based on the collected results, the ship responses for a series of sea states characterized by JONSWAP wave spectra with significant wave height from 0 to 10 m, peak period from 4 to 15 s and wave headings from 0° (following seas) to 180° (head waves) have been evaluated and stored in a database to be used by the routeing tool. Wind resistance is calculated using Blendermann's coefficients (Blendermann 1994).

Using the results obtained by the above methods, the routeing tool can evaluate the ship's total resistance at any point of its route, based on the weather predictions at the specific point and time and for the assumed ship speed and heading. Then, the required propulsion power can be readily calculated, based on the available propeller curves. The specific fuel oil consumption (SFOC) is then calculated, based on data provided by the engine manufacturer.

To demonstrate the potential of the weather routeing tool, results from the optimization of a crossing of the Atlantic Ocean with the vessel assumed at its design draught will be presented in the following. The vessel exits the Mediterranean from the Strait of Gibraltar, heading towards Halifax, Nova Scotia. The crossing is assumed to start on 06/01/2018 and the ship should arrive at its destination within 144 h. The minimum[4] distance of the voyage is 2373.5 nm and with the specified crossing duration can be travelled at an average speed of 16.7kn. The route optimization is based on weather forecasts provided by Copernicus Marine Environment Monitoring Service and is carried out via the genetic algorithm solver, available in Matlab's® optimization toolbox, using a population size of 200 and 100 generations. Mutation and crossover functions are used to provide genetic diversity, to enable the genetic algorithm to search a broader space and to ensure that feasible parents give rise to feasible children, where feasibility is with respect to bounds. The objective of the optimization was the minimization of fuel consumption, subject to the following set of constraints:

[4]The distance corresponding to the great circle between the departure and arrival points.

- Travel time no more than 144 h
- Significant vertical acceleration at the bridge of the ship:
  - between 0.30 g and 0.45 g for not more than 12 h
  - between 0.45 g and 0.60 g for not more than 10 h
- Significant vertical acceleration at the bow of the ship:
  - between 0.70 g and 0.80 g for not more than 12 h
  - between 0.80 g and 0.90 g for not more than 10 h
- Significant roll angle:
  - from 8 to 10° for not more than 6 h
  - from 10 to 14° for not more than 2 h

Thirteen optimization variables were used, consisting of the coordinates (longitude and latitude) of four intermediate waypoints and the speed of the vessel along each one of the 5 voyage legs. The optimization was carried out for 100 generations, resulting in 20,000 voyage alternatives, 668 of which were feasible. The evolution of the fuel oil consumption is illustrated in Fig. 8.16. As can be observed from this figure, the members of the initial generations are characterized by extremely high FOC, while improved results are obtained gradually, and finally a large number of voyages are identified with a FOC below 240 t.

The key point in order to reduce the FOC is to navigate the vessel in a way that avoids the most severe wave conditions during the crossing. This is evident from the following figures (Figs. 8.17, 8.18 and 8.19) where the fuel oil consumption is plotted against the total number of hours during the crossing for which the vessel responses are kept within the specified limits (i.e. significant vertical acceleration at the bridge and at the ship bow less than 0.30 g and 0.70 g respectively and significant roll angle less than 8°).

The route minimizing FOC, while fulfilling the specified constraints was found in the 100th generation. The route length is equal to 2390.6 nm and the calculated FOC is equal to 237.83 tons. The FOC along the optimal route is 5 tons less (2% reduction) than the FOC calculated for the vessel sailing along the great circle (i.e.

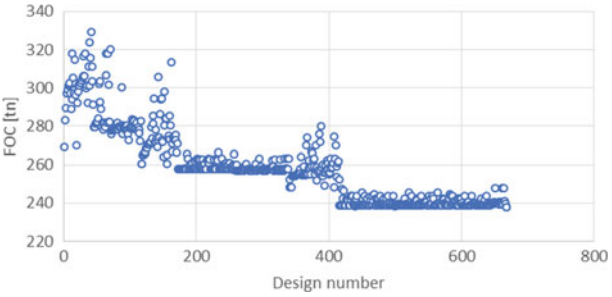

Fig. 8.16 Evolution of fuel oil consumption (only feasible voyages shown)

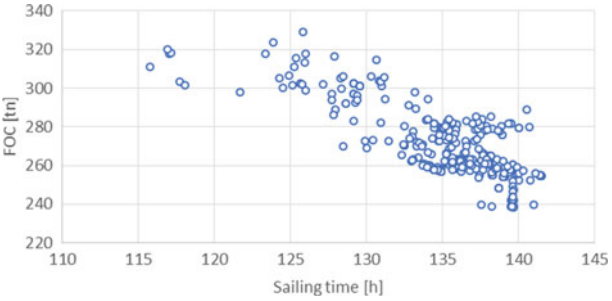

Fig. 8.17 Aggregate time during sailing with significant vertical bridge acceleration not greater than 0.30 g

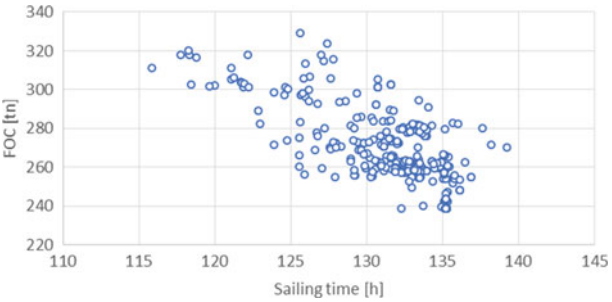

Fig. 8.18 Aggregate time during sailing with significant vertical bow acceleration not greater than 0.70 g

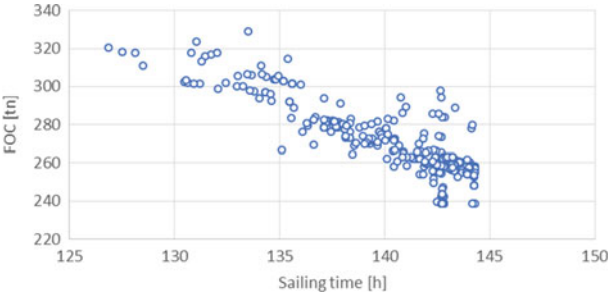

Fig. 8.19 Aggregate time during sailing with significant roll angle not greater than 8°

along the route minimizing the distance between the departure and destination points, also known as the orthodrome). The distance along the great circle is 2373.5 nm, i.e. 17.1 nm less than that of the optimal route. In addition, the FOC along the optimal route is 5.9 tons less (2.4% reduction) than the FOC calculated for the vessel following the rhumb line (i.e. along the route with constant heading between the departure and destination points, also known as the loxodrome, shown as a straight

line in a Mercator projection). The distance along the rhumb line is 2399.1 nm, i.e. 8.5 nm more than that of the optimal route and 25.6 nm more than the great circle. The reduction in FOC obtained by the route optimization is relatively small, it should be noted however, that the above mentioned FOC along the great circle and the rhumb line have been obtained by a systematic speed optimization along each route using the same weather routeing tool. These optimizations were carried out in order to bring the ship responses along these routes within the specified constraints, while the achieved fuel oil consumption was just a side effect. Without the speed optimization, sailing along the great circle or the rhumb line (for example with constant speed) resulted in significant violation of the specified seakeeping constraints.

The trajectory of the optimal route with a step of 24 h (the time of departure appearing top left) plotted against the prevailing significant wave height prediction at each instant is presented in Fig. 8.20. At the bottom-right plot of Fig. 8.20 the optimal route (green line) is compared with the great circle and the rhumb line, (appearing as a circular ark and a straight line in a Mercator projection respectively, both in red colour).

8.6 Conclusions

The outcome of the work that was carried out on the operational optimization and hull form retrofitting of two widely used vessel types, namely a bulk carrier and a container ship was presented. For both vessels, trim optimization was carried out using advanced CFD tools, while the required propulsion power reduction by systematic bulbous bow optimization was also investigated. In addition, a ship routeing tool was developed and applied to both vessels's operation using realistic operational conditions and online weather data, aiming to reduce fuel oil consumption, while keeping set margins for travel time and seakeeping criteria.

For both vessels, trim optimization studies indicated that it is possible to reduce calm water resistance and required propulsion power by a bow down trim angle. For the original hull form of the bulk carrier (the hull without the bulbous bow), the optimum trim angle at design speed (14.5 kn) minimizing the calm water propulsion power is equal to 0.25°. At this trim angle, the calm water propulsion power is reduced by approximately 1% in comparison with the power required at level trim. The corresponding optimum trim angle for the container ship is found in the range between 0.23° to 0.35°, depending on the ship speed. The propulsion power reduction ranges between 2 and 3%, depending on speed.

Fitting of a bulbous bow on the bulk carrier can reduce the propulsion power by approximately 1%, both at level trim, and with a bow down trim between 0.125° and 0.25°. For container ship at the specified speed of 18 kn, a reduction of propulsion power by a bulbous bow optimization in the order of 3% was obtained with the vessel at zero trim and up to 4% with a bow down trim angle of 0.23° (1 m trim by the bow). The positive impact of bow down trim on the resistance and propulsion might be attributed to the reduction of the immersed area of the transom.

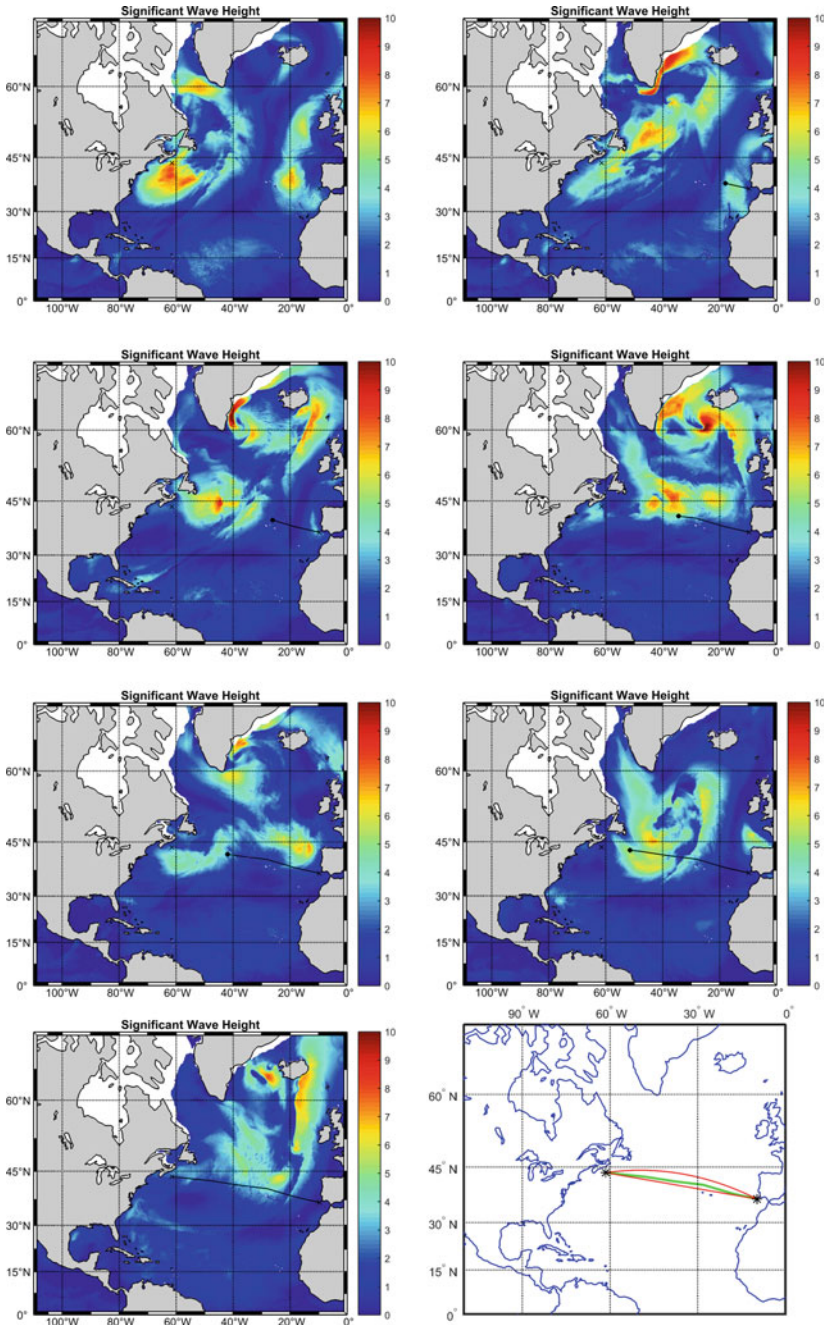

Fig. 8.20 Distance travelled per day against the significant wave height and comparison of optimal route (green) with great circle and rhumb line (both in red)

Given that the original hull forms of both vessels have been already extensively optimized by the shipbuilders, the obtained improvements may be considered quite satisfactory, particularly for the container ship.

Weather routeing optimization studies for both vessels resulted in a reduction of the fuel consumption in the order of 2% in comparison with the fuel consumption obtained when sailing along the great circle (despite the increase of the route length and the average speed) and in the order of 2.4% in comparison with the fuel consumption obtained when sailing along the rhumb line (i.e. along the route with constant heading between the departure and destination points, shown as a straight line in a Mercator projection). It should be noted however, that the fuel oil consumption along the great circle and the rhumb line which are compared with that along the optimum route have been both obtained by a systematic speed optimization along each route using the same weather routeing tool. These optimizations were carried out in order to keep ship responses along these routes within the specified constraints, while the achieved fuel oil consumption was just a side effect. Without the speed optimization, sailing along the great circle or the rhumb line (for example with constant speed) resulted in significant violation of the specified seakeeping constraints. The obtained results indicated that even if the fuel oil savings are not quite high, the obtained reduction of the vessel's responses (in this particular case the vertical acceleration at the bridge and at the bow and the roll angle) may be particularly significant, improving the quality of the crossing and enhancing the safety of the ship and cargo (e.g. minimization of the risk of lost deck containers). It should be also noted that the studied ships are quite large in absolute size and it may be expected that similar studies on smaller vessels on the same route would result in more striking impact.

Based on the obtained results, it may be concluded that optimization methods, when properly applied can be valuable tools both for the hull retrofitting and for the improvement of ship operation. Cumulative savings obtained by the combined effect of carefully optimized hullform retrofitting and operational optimization can become quite substantial, resulting in significant reduction of fuel consumption and greenhouse gas emissions along with significantly improved ship responses in the waves.

References

Abt, C., & Harries, S. (2007). A New Approach to Integration of CAD and CFD for Naval Architects. 6th *International Conference on Computer Applications and Information Technology in the Maritime Industries (COMPIT 2007a)*, Cortona, Italy, April 2007.

Abt, C., Harries, S., Wunderlich, S., & Zeitz, B. (2009). Flexible tool integration for simulation-driven design using XML, generic and COM interfaces. 8th *International Conference on Computer Applications and Information Technology in the Maritime Industries (COMPIT 2009)*, Budapest, Hungary, May 2009.

Blendermann, W. (1994). Parameter Identification of Wind Loads on Ships. *Journal of Wind Engineering and Industrial Aerodynamics*, pp. 339–351.

Deng, G. B., Guilmineau, E., Queutey, P., & Visonneau, M. (2005). Ship Flow Simulations with the ISIS-CFD Code. CFD Workshop Tokyo 2005, T. Hino (Ed.), Tokyo, pp. 474–482.

Deng, G. B., Leroyer, A., Guilmineau, E., Queutey, P., Visonneau, M., Wackers J., & del Toro Llorens, A. (2015). Verification and validation of resistance and propulsion computation. Proceedings of Tokyo 2015 Workshop on CFD in Ship Hydrodynamics.

Gatchell, S., Hafermann, D., Jensen, G., Marzi, J., & Vogt, M. (2000). Wave resistance computations—A comparison of different approaches. In 23rd *Symposium on Naval Hydrodynamics*, 17–22 September, Val de Reuil, France.

Hafermann, D. (2007). The New RANSE Code FreSCo for Ship Applications, STG Jahrbuch.

Harries, S., & Abt, C. (2018). CAESES®—The HOLISHIP Platform for Process Integration and Design Optimization, In: Apostolos Papanikolaou (Ed.) A Holistic Approach to Ship Design, Volume 1: Optimisation of Ship Design and Operation for Life Cycle, ISBN 978–3–030–02809–1 (print) 978–3–030–02810–7 (ebook), Springer Nature Switzerland.

Kallos, G. (1997). The regional weather forecasting system SKIRON. *Proceedings of the Symposium on Regional Weather Prediction on Parallel Computer Environments*.

Liu, S., Papanikolaou, A., & Zaraphonitis, G. (2011). Prediction of added resistance of Ships in waves. *Ocean Engineering, 38*, 641–650.

Liu, S., Papanikolaou, A., & Zaraphonitis, G. (2015). Practical approach to the added resistance of a ship in short waves. *Proceedings Ocean (Offshore) and Polar Engineering Conference (ISOPE)*, Hawaii, USA.

Liu, S. K., & Papanikolaou, A. (2015). Fast approach to the estimation of the added resistance of ships in head waves. *Journal Ocean Engineering, 112*(216), 211–225. https://doi.org/10.1016/j.oceaneng.2015.12.022.

Marzi, J., Papanikolaou, A., Corrignan, P., Zaraphonitis, G., & Harries, S. (2018). HOLISTIC ship design for future waterborne transport. Proceedins 7th Transport Research Arena, TRA 2018, April 16–19, 2018, Vienna, Austria.

Papanikolaou, A, & Zaraphonitis, G. (1987). On an improved method for the evaluation of second-order motions and loads on 3D floating bodies in waves. *Journal Schiffstechnik-Ship Technology Research, 34*, 170–211.

Papanikolaou, A, & Schellin, Th. (1992). A three-dimensional panel method for motions and loads of ships with forward speed. *Journal Schiffstechnik—Ship Technology Research, 39*(4), 147–156.

George Zaraphonitis studied Naval Architecture and Marine Engineering at the National Technical University of Athens (NTUA). He received his Ph.D. from the School of Naval Architecture and Marine Engineering of NTUA in 1990. From 1993 to 1998 he worked at the Eleusis Shipyards and at MARTEDEC S.A. in Piraeus. He is currently Professor of Ship Design at the School of Naval Architecture and Marine Engineering of NTUA. His research interests include ship design and optimization, ship safety, design of advanced marine vessels, ship hydrodynamics.

Aggeliki Kytariolou received her diploma in Naval Architecture and Marine Engineering from NTUA in October 2016. She joined the Ship Design Laboratory (NTUA) in 2017 as a researcher and she is also a PhD student. Her main interests are in the fields of seakeeping, weather routeing and ship design optimization.

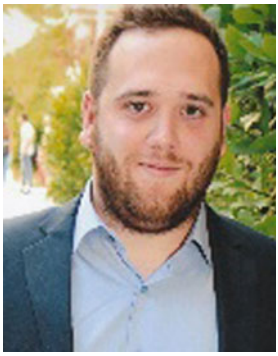

George Dafermos received his diploma in Naval Architecture and Marine Engineering from the National Technical University of Athens (NTUA) in February 2016. After his graduation he joined the Ship Design Laboratory-NTUA as a researcher, while at the same time he is pursuing PhD studies on the dynamics of ships in damaged condition. He has participated in various EU-funded research projects. His primary interests are in the fields of seakeeping in intact and damaged condition, damage stability assessment and ship design optimization.

Scott Gatchell received his BSE (1997) and MSE (1999) in Naval Architecture and Marine Engineering from the University of Michigan. Since that time, he has worked in the CFD department of HSVA, participating in several national and international research projects involving ship hydrodynamics.

Anders Östman Research scientist in SINTEF Ocean since 2009. Wide CFD expertise developed in the following topics: vessel performance in calm water, added resistance, PMM simulations, modeling of hull roughness, and simulation of extreme wave impact events on offshore structures.